HHS Public Access

Author manuscript

J Cell Physiol. Author manuscript; available in PMC 2019 January 01.

Published in final edited form as:

J Cell Physiol. 2018 January ; 233(1): 11–22. doi:10.1002/jcp.25882.

Plasma Membrane Calcium ATPase 4 (PMCA4) co-ordinates Calcium and Nitric Oxide signaling in regulating Murine Sperm functional activity

Kristine E. Olli, **Kun Li**[2], **Deni S. Galileo**, and **Patricia A. Martin-DeLeon**[1,*]

[1]Department of Biological Sciences, University of Delaware, Newark, DE 17916

Abstract

Reduced sperm motility (asthenospermia) and resulting infertility arise from deletion of the *Plasma Membrane Ca^{2+}-ATPase 4 (Pmca4)* gene which encodes the highly conserved Ca^{2+} efflux pump, PMCA4. This is the major Ca^{2+} clearance protein in murine sperm. Since the mechanism underlying asthenospermia in PMCA4's absence or reduced activity is unknown, we investigated if sperm PMCA4 negatively regulates nitric oxide synthases (NOSs) and when absent NO, peroxynitrite, and oxidative stress levels are increased. Using co-immunoprecipitation (Co-IP) and Fluorescence Resonance Energy Transfer (FRET), we show an association of PMCA4 with the NOSs in elevated cytosolic [Ca^{2+}] in capacitated and Ca^{2+} ionophore-treated sperm and with neuronal (nNOS) at basal [Ca^{2+}] (ucapacitated sperm). FRET efficiencies for PMCA4-eNOS were 35% and 23% in capacitated and uncapacitated sperm, significantly ($P<0.01$) different, with the molecules being <10 nm apart. For PMCA4-nNOS, this interaction was seen only for capacitated sperm where FRET efficiency was 24%, significantly ($P<0.05$) higher than in uncapacitated sperm (6%). PMCA4 and the NOSs were identified as interacting partners in a quaternary complex that includes Caveolin1, which co-immunoprecipitated with eNOS in a Ca^{2+}-dependent manner. In *Pmca4*$^{-/-}$ sperm NOS activity was elevated 2-fold in capacitated/uncapacitated sperm (versus wild-type), accompanied by a 2-fold increase in peroxynitrite levels and significantly ($P<0.001$) increased numbers of apoptotic germ cells. The data support a quaternary complex model in which PMCA4 co-ordinates Ca^{2+} and NO signaling to maintain motility, with increased NO levels resulting in asthenospermia in *Pmca4*$^{-/-}$ males. They suggest the involvement of *PMCA4* mutations in human asthenospermia, with diagnostic relevance.

Keywords

oxidative stress; infertility; sperm damage; calcium efflux pump; asthenospermia

[*]Corresponding author: 219 Mckinly Lab, Univ. Delaware, Newark DE 19716, Tel: 302-831-2249, Fax: 302-8312281, pdeleon@udel.edu.

[2]Current address: Department of Reproductive Physiology, Zhejiang Academy of Medical Sciences, Hangzhou, Zhejiang 310013, China.

Introduction

Capacitation is the series of changes that occur in the final maturation of mammalian sperm in the female in order for them to gain fertilizing competence, and subsequently undergo the acrosome reaction. Both of these processes are dependent on elevated levels of cytosolic Ca^{2+} concentration ($[Ca^{2+}]_c$) (de Lamirande et al., 1997; Fraser 1987). After the calcium influx required to meet this high calcium demand, there needs to be a return to resting cytosolic calcium concentration ($[Ca^{2+}]_c$) levels [50–100 nM (Herrick et al., 2005)]. In mice, in the absence of the major calcium efflux pump, Plasma Membrane Calcium ATPase 4 (PMCA4) (Wennemuth et al., 2003), calcium levels remain elevated with loss of sperm motility (Asthenospermia, AS) and resulting male infertility (Okunade et al., 2004; Schuh et al., 2004). The highly conserved PMCA4 in murine sperm is known to share an interacting partner, CASK (Ca^{2+}/CaM-dependent serine kinase), with Junctional adhesion molecule A (JAM-A) (Aravindan et al., 2012). We have reported AS in mice lacking *Jam-A* (Shao et al., 2008) and have shown that it is associated with decreased activity of PMCA4 (Aravindan et al., 2012).

To date the underlying mechanism responsible for the loss of sperm motility resulting from PMCA4's absence, or its reduced activity, has not been elucidated. So far, PMCA4's only interacting partner identified in sperm is CASK to which it binds preferentially at basal cytosolic Ca^{2+} concentration ($[Ca^{2+}]_c$) in uncapacitated cells, via its C-terminal PDZ-ligand (Aravindan et al., 2012). This is consistent with the known PMCA4-CASK interaction in somatic cells in low intracellular Ca^{2+} microdomains (Schuh et al., 2003; Oceandy et al., 2007). On the other hand JAM-A-CASK interaction facilitates Ca^{2+} efflux, since in its absence in *Jam-A* null sperm $[Ca^{2+}]_c$ is elevated (Aravindan et al., 2012). Since CASK has only a single PDZ domain where it is also known to bind to JAM-A (Aravindan et al., 2012), both PMCA4 and JAM-A cannot bind to CASK simultaneously and likely bind sequentially. Thus it is important to ask to what does PMCA4 bind when the basal $[Ca^{2+}]_c$ is elevated in capacitated or acrosome-reacted sperm?

Apart from its known function of regulating calcium homeostasis (Di Leva et al., 2008), PMCA4 can regulate NO signaling by controlling the NOSs (Holton et al., 2010; Schuh et al., 2001). In neuronal cells PMCA4, via its PDZ ligand, is known to interact with nNOS to negatively regulate it (Schuh et al., 2001). Similarly, it negatively regulates eNOS in endothelial cells, via an interaction with its catalytic domain (Holton et al., 2010). Thus both of these constitutive NOSs are able to interact with PMCA4 simultaneously. Recently, we showed that in human sperm these interactions are Ca^{2+}-dependent (Andrews et al., 2015). We hypothesize that both NOSs are tethered to PMCA4 preferentially in capacitated mammalian sperm when there is an influx of Ca^{2+} (Fraser, 1987; de Lamirande et al., 1997) which rapidly activates them (Knowles and Moncada, 1994). Thus as PMCA4 extrudes Ca^{2+}, the NOSs are held in a locale or microdomain with a relatively low $[Ca^{2+}]_c$, compared to the surrounding environment where it is globally high. In this Ca^{2+}-extruding locale, NOS activity is inhibited and this prevents non-physiologically high levels of NOS activity and NO.

Based on the above hypothesis, in *Pmca4* null sperm as well as in *Jam-A* nulls (where PMCA4 activity is significantly reduced), negative regulation of the NOSs would be absent or decreased and thus the levels of NO would be significantly elevated. As a consequence, there would be elevated levels of peroxynitrite ($OONO^-$), a primary effector of NO, which is produced when NO combines with superoxide (O_2^-). While physiological levels of ($OONO^-$) play an important role in capacitation (Herrero et al., 2001), elevated levels are toxic due to its highly reactive nature and therefore could lead to lipid peroxidation which is a key factor in loss of sperm motility (Aitken et al., 2014; Hellstrom et al., 1994).

Thus the goal of this investigation was to determine if: 1) in murine sperm the NOSs are interacting partners of PMCA4 and if they interact in a Ca^{2+}-dependent manner, as they do in human sperm, 2) *Pmca4* null sperm have elevated levels of NO and peroxynitrite, a highly reactive oxygen species (ROS), and 3) the level of apoptosis is increased in *Pmca4* null germ cells, compared to those of wild-type (WT) littermates.

Materials and Methods

Animals and Reagents

Sexually mature (>3 months old) male mice of the C57BL/6, FVBN, or ICR backgrounds (Harlan Sprague-Dawley, Indianapolis, IN) were used in the studies. *Pmca4* KO males on the FVBN background were generated from the matings of *Pmca4* +/− donated by the Shull laboratory (Okunade et al., 2004). Breeding and genotyping of these mice were described previously (Okunade et al., 2004). *Jam-A* null sperm were generated and genotyped as described (Shao et al., 2008). The studies performed were approved by the Institutional Animal Care and Use Committee (IACUC) at the University of Delaware and were in agreement with the Guide for the Care and Use of Laboratory Animals published by the National Academies, 8th ed., Washington, DC (publication 85–23, revised 2011). All chemicals were purchased from Fisher Scientific Co. (Malvern, PA) or Invitrogen or Life technologies (Carlsbad, CA) unless otherwise specified.

Antibodies

The following antibodies were purchased from Santa Cruz Biotechnology (Dallas, TX): 1) affinity purified goat polyclonal PMCA4 antibody (Y20, sc-22080; recognizes both 4a and 4b isoforms) raised against the N-terminus of the rat protein, 2) a mouse monoclonal PMCA1/4 (5F10) antibody (sc-20028) with the epitope mapping to amino acids 719–738 of human PMCA4b, 3) rabbit polyclonal anti-eNOS antibody (NOS3, C20; sc- 654) whose epitope maps at the C-terminal end of human NOS3, and 4) rabbit polyclonal anti-nNOS antibody (NOS1, R20; sc-648). A rabbit polyclonal anti-CAV-1 (Caveolin 1) antibody was obtained from BD transduction Laboratories (San Jose, CA). Secondary antibodies were purchased from Life Technologies, Santa Cruz Biotechnology, or Molecular Probes Inc. (Eugene, OR). These antibodies were used in Western blots, co-immunoprecipitation assays, indirect immunofluorescence, and FRET studies, all of which demonstrated their specificity in detecting these proteins in mice.

Sperm Collection and Protein Extraction

Males were sacrificed by CO_2 asphyxiation, according to IACUC, and the caudal epididymal tissue collected in Human tubal fluid (HTF, InvitroCare, Frederick, MD) which contains 2 mM calcium. The tissue was then minced and incubated at 37°C for 10 min to release sperm. The sperm suspensions were separated from the tissue by gravity settling and sperm were recovered by centrifugation 500 × *g* for 20 min. Following centrifugation, samples were processed immediately as uncapacitated sperm, or either incubated for 90–120 min in HTF medium at 37°C to undergo capacitation, or treated with 1μM A23187 calcium ionophore and incubated at 37°C for 65 min to undergo the acrosome reaction (Deng et al., 1999; Al-Dossory et al., 2015). Capacitated and acrosome-reacted sperm were collected by centrifugation at 500 × *g* for 20 min.

Proteins were extracted from sperm as previously described (Zhang and Martin-DeLeon, 2003) in Homogenization Buffer (HB, 62.5 mM Tris-HCl, 10% glycerol, 1% SDS) or RIPA buffer with Protease Inhibitor (PI) (Sigma Aldrich, St. Louis, MO) and the tubes rotated overnight at 4°C. The suspension was then centrifuged at 14,000 × *g* for 15 min, and the protein extract was collected in the supernatant. The protein concentration was determined using the Pierce bicinchoninic acid (BCA) assay kit (Thermo Scientific, Rockland, IL).

Co-Immunoprecipitation (Co-IP) Assays

Sperm protein extracts were used for co-immunoprecipitation assays as previously described from our Lab (Aravindan et al., 2012; Modelski et al., 2014). Briefly, 50 μl of PureProteome Protein G Magnetic Beads (Millipore Corp, Billerica, MA) were washed twice with 1 ml PBS + 0.01% Tween 20 by vortexing, and recovered by centrifugation at 2500 × *g* for 5 min. They were then re-suspended in 100 μl of PBS with 2 μg of the specific antibodies (anti-PMCA4, anti-PMCA1/4, anti-eNOS, or anti-nNOS) for 2 h on a rotator at 4°C, while the control received the same concentration of appropriate IgG (goat for PMCA4, mouse for PMCA1/4, and rabbit for the NOSs). After incubation, the beads were centrifuged at 2500 × *g*, the supernatant removed prior to washing them with PBS. The beads were then re-suspended in 105–125 μg of sperm protein extract in immunoprecipitation buffer (IP buffer: 25 mM Tris, 150 mM NaCl, pH 7.2) and PI for a total of 500 μl, and the samples were rotated overnight at 4°C. The beads were then recovered by centrifugation at 2500 × *g* for 5 min and washed twice in PBS before solubilizing in 20 μl RIPA buffer. Loading dye (5 μl of a 5× solution) was added and the beads re-suspended prior to preparation for SDS-PAGE.

SDS-PAGE and Western Blot Analysis

Western blotting was performed to detect an interaction between nNOS and PMCA4 and eNOS and PMCA4 in the protein extracts. The bead suspension with the loading dye was subjected to reducing conditions of 100°C for 5 min to elute the proteins for analysis on SDS-PAGE (8%). Proteins were then transferred to nitrocellulose membrane (Amersham Biosciences) according to standard protocols. Membranes were probed at 4°C for 24–48 h with either rabbit polyclonal antibodies specific to nNOS (1:500), eNOS (1:250), CAV-1 (1:1000), or goat polyclonal antibody specific to PMCA4 (1:500), or mouse monoclonal PMCA1/4 (1:400) that detects both PMCA4 and PMCA1 which are present in mouse sperm

in a 9:1 ratio (Okunade et al., 2004). They were then washed three times with TBST (20 mM Tris, pH 8.0 containing 150 mM NaCl, and 0.5% Tween 20) for 10 min each.

The secondary antibody for membranes probed with anti-PMCA4 was 1:5000 biotin donkey anti-goat (Jackson Laboratory, West Grove, PA), After 30 min exposure at RT blots were washed 3× with TBST for 10 min each. A dilution of 1:5000 Streptavidin Horse Radish Peroxidase (SA-HRP) (Jackson Laboratory, West Grove, PA) was added to the membrane for 30 min at RT, followed by 3 washes with TBST at RT for 5 min and then with double-distilled water twice for 5 min each at RT. The secondary antibody for anti-panPMCA was alkaline phosphatase (AP)-conjugated anti-mouse IgG, 1:2000, (Invitrogen). Bands were visualized using a WesternBreeze Chemiluminescent Immunodetection kit (Invitrogen, Carlsbad, CA) or the ECL kit (Bio-Rad, Hercules, CA).

In the reciprocal Co-IP, membranes probed with anti-eNOS or anti-nNOS were first washed 3× with TBST for 10 min at RT, then the proteins were detected with either AP- conjugated anti-rabbit secondary antibody or with Multilink secondary antibody (1:5000) from Biogenex, Fremont, CA). If they were probed with AP-conjugated anti-rabbit IgG, Immuno-Star AP substrate and Enhancer were used to visualize the bands. For the Multilink secondary, bands were visualized using the WesternBreeze Chemiluminiscent Immunodetection kit.

Indirect Immunofluorescence of Proteins in Murine Sperm—Proteins were studied in both capacitated and uncapacitated sperm, as prepared above. Sperm pellets were re-suspended in 4% paraformaldehyde and incubated overnight at 4°C for fixation. The samples were recovered by centrifugation at 500 × *g* for 15 min and washed twice in PBS before permeabilization in 0.1% Triton X-100 in PBS at RT for 10 min. The cells were then collected by centrifugation and after washing in PBS were re-suspended in blocking buffer (2% Bovine Serum Albumin in 1× PBS), washed, and blocked at RT for 30 min. After blocking, the pellets were reconstituted and aliquotted into two tubes (control and test). The test tubes were incubated in primary antibodies: anti-PMCA4, anti-nNOS, anti-eNOS, each at a dilution of 1:50 and the control in the same concentration of IgG (goat and rabbit where appropriate) at 4°C overnight.

After incubation, cells were collected by centrifugation and washed 3× with PBS before incubation with secondary antibodies: Alexa Fluor 555-conjugated donkey anti-goat IgG for PMCA4 and Alexa Fluor 488-conjugated goat anti-rabbit IgG for eNOS and nNOS, all diluted 1:200. After 30 min at RT in the secondary antibodies in the dark, samples were washed 3× with PBS and the pellets reconstituted in 40 μl of PBS. Approximately 20 μl of the cell suspension were layered onto a coverslip with 50 μl of prolong gold antifade reagent with DAPI and carefully laid onto a Colorfrost Plus Microscope Slides and cured at 4°C for 24 h. After sealing the edges, slides were stored at 4°C before confocal microscopy.

Co-localization and Fluorescence Resonance Energy Transfer (FRET) via Acceptor Photobleaching—Slides were prepared as described above, with the following alterations. The primary antibodies were added in pairs, PMCA4 and eNOS, and PMCA4 and nNOS. Secondary antibodies were also added in sets corresponding to the respective

primary antibodies. Slides were visualized using a Zeiss LSM 780 confocal microscope and analyzed using ZEN software.

FRET was used to study molecular scale interactions between PMCA4/eNOS and PMCA4/nNOS. This was performed identically to that recently described in our Lab for human sperm (Andrews et al. 2015). In this technique an excited donor fluorophore transfers its energy to a light-absorbing acceptor molecule if the molecules are closer than ~100 Å. The Acceptor Photobleaching approach described by Bragdon et al. (2009, 2010) was used to evaluate FRET efficiencies. For this, a donor fluorophore (green label, Alexa Fluor 488, which excites at 488 nm and emits at 519 nm) was used to tag eNOS and nNOS and an acceptor fluorophore (red, Alexa Fluor 555, which excites at 561 nm and emits at 565 nm) was used for PMCA4. The Forster distance (R0, the distance at which energy transfer efficiency is 50% of the maximum possible for a particular donor-acceptor) for Alexa Fluor 488 and Alexa Fluor 555 is known to be 70 Å (Life Technologies). With the occurrence of FRET the donor encounters a quenching of its fluorescence due to the energy transfer to the acceptor. However after photobleaching of the acceptor, donor fluorescence is not quenched, but rather increased in intensity. The difference between the average fluorescence intensities of the donor post- and pre-bleaching divided by the average post-bleach intensity provides a direct assessment of the FRET efficiency. If this value exceeds 20%, the two molecules tagged are considered within 10 nm of each other (Bragdon et al., 2009).

To obtain the data, lasers were used to excite the fluorophores and a region of interest (ROI) encompassing a sperm was selected and 5 initial images of the donor fluorophore were taken. Following the bleaching event which consisted of 40 iterations of the laser, to ensure that the acceptor was completely bleached and that there would be maximal enhancement of the donor, 15 more images were captured. Thus, there were a total of 20 images/cell. These high resolution and high magnification images were collected, using confocal microscopy (with a Zeiss LSM 780 confocal microscope; Carl Zeiss Inc, Gottingen, Germany) with a plan-Apochromatic 63× oil objective and the FRET module.

The area of the ROI was calculated and normalized for the intensity values for pre- and post-bleach, using Image J (U.S. National Institute of Health, Bethesda, MD, USA). Also, using Image J, the background fluorescence was calculated and subtracted from the pre- and post-intensity values. For PMCA4/eNOS there were a total of 4 treatment groups of sperm analyzed: 2 of which were uncapacitated (UNCAP), pre- and post-bleaching and 2 were capacitated (CAP), pre- and post-bleaching. Similarly, for PMCA4/nNOS there were 4 groups in the categories described for PMCA4/eNOS. In each of the 4 groups for each of the two protein pairs, there were 10 cells.

Determination of NOS activity in Pmca4 and Jam-A nulls—Using a real-time assay, NOS activity (reflecting NO bioavailability) was measured in nulls and WT live sperm, capacitated and uncapacitated, with the NOS Detection kit (Cell Technology Inc., Mountain View, CA). The assays were performed according to the manufacturer's instructions. Briefly, in the assay the production of NO converts a non-fluorescent dye into its fluorescent derivative that can be observed by excitation at 488 nm and the measurement of emission at 515 nm. Equal numbers of sperm were incubated with the dye for 60 min in

the dark at RT before FACScan analysis was used to detect activity in 50,000 cells per sample.

Determination of Reactive Oxygen Species (ROS) in Pmca4 Null Sperm—The level of oxidative stress from elevated levels of OONO- resulting from NOS activity was investigated, using a ROS Detection kit (Cell Technology Inc., Mountain View, CA). This kit detects highly reactive oxygen species, such as peroxynitrite (OONO-), with the hydroxyl phenyl fluorescein (HPF) probe. The probe was diluted 1:130 according to the manufacturer's instructions and as described (Setsukinai et al., 2002). FACScan analysis (excitation at 488 nm, emission at 515 nm) was used to determine the levels of ROS, as detected by fluorescence intensity, in WT and null sperm, capacitated and uncapacitated.

TUNEL Assay for the Detection of Apoptosis in Pmca4 Null Testicular Tissue —Testes from three (3) sexually mature mice, WT and three *Pmca4* nulls, were placed into Tissue-Tek Cryomold (Sakura, Torrance, CA) with optimum cutting temperature (OCT) medium. (Sakura, Torrance, CA), then on dry ice before freezing at −80°C. Frozen sections were routinely prepared. TUNEL assays were performed on frozen sections with the ApopTag Fluorescein *In Situ* Apoptosis Detection Kit (Cat.# S7110, Millipore) according to the manufacturer's instructions.

Sections on slides were post-fixed in pre-cooled ethanol: acetic acid (2:1) for 5 min at −20°C in a coplin jar and washed twice in PBS for 5 min. After processing, slides were incubated in TdT (terminal deoxynucleotidyl transferase) enzyme in a humidified chamber at 37°C for 1 h. Slides were washed in PBS and then incubated in anti-digoxigenin-fluorescein for 30 min. They were then washed and counter-stained with DAPI, and coverslipped. Slides were stored at −20°C until analyzed and imaged, using a confocal microscope. The numbers of apoptotic cells in 100 tubules and their location were blindly recorded for each group.

Statistical Analysis

The data for the sperm groups in the FRET analysis were statistically analyzed using one-way ANOVA and the Student's *t*-test was performed to calculate significant differences in the FRET efficiency between treatment pairs. The Student *t-test* was also used for analysis of the differences in the number if apoptotic cells in WT and *Pmca4* null males. The threshold for significance was a P value <0.05. However, P values substantially less than 0.05 were reported to denote the level of significance.

Results

To date, localization of the NOSs in murine sperm has not been established, unlike PMCA4 which has been shown to reside over the acrosome and on the proximal principal piece (Wennemuth et al., 2003; Aravindan et al., 2012). In Fig. 1A we show that both NOSs localize to the head, and the flagellum. However, the distribution on the flagellum is dissimilar with the far more abundant nNOS localized to the midpiece, the proximal principal piece, and the distal principal piece. On the other hand, eNOS is found only on the midpiece and the proximal principal piece.

To determine if PMCA4 and nNOS are physically associated in a complex which is Ca^{2+} – dependent, reciprocal Co-IP assays were performed on proteins from sperm that were uncapacitated (UNCAP) with low basal $[Ca^{2+}]_c$, and capacitated (CAP) and acrosome-reacted (AR) sperm where $[Ca^{2+}]_c$ is elevated. The latter was achieved with Ca^{2+}ionophore treatment under conditions in which >90% of the sperm population was shown to be acrosome–reacted (Deng et al., 1999). Our results show that anti-nNOS antibodies were able to co-immunoprecipitate PMCA4 in proteins from all three groups of sperm with the UNCAP band being the strongest (Fig. 1B). The ~133 kDa PMCA4 band is seen in the total protein used as a positive control, but absent in the IgG control. When anti-PMCA4 antibodies were used for Co-IP, the Western blots showed a more intense 155 kDa nNOS band in proteins from CAP, compared to UNCAP, cells (Fig. 1B). In Fig. 1C, anti-eNOS antibodies co-immunoprecipitated an ~133 kDa PMCA4 band in CAP, but not UNCAP, sperm with total protein and IgG being positive and negative controls. The interaction between eNOS and PMCA4 was confirmed in the reciprocal Co-IP which included Ca^{2+} ionophore-treated AR samples. Both AR and CAP sperm showed the 140 kDa eNOS band, indicating an association between PMCA1/4 (panPMCA) and eNOS, with the AR band being stronger than that of the CAP. There were no bands for UNCAP or the negative IgG control.

Since in somatic cells the eNOS-Caveolin1 (CAV-1) system in lipid rafts is well-established as regulating NOS activity (Dhillon et al., 2003) and since in murine sperm PMCA4 (Aravindan et al., 2012) and CAV-1 (Travis et al., 2001) have been localized in lipid rafts, we asked if CAV-1 may also be interacting with the PMCA4-eNOS complex. In Fig. 1D we show that when eNOS was co-immunoprecipitated with anti-PMCA4 antibodies and the membrane stripped and re-probed with anti-CAV-1, CAV-1 (24 kDa) was detected in the total protein and above control levels only at high $[Ca^{2+}]_c$ in CAP sperm. In Fig. 1D (right) with only proteins from CAP sperm assayed, the blot for CAV-1 shows a strong band with the anti-PMCA4 antibodies, but none for the IgG control. The simultaneous Co-IP of eNOS and CAV-1 with anti-PMCA4 antibodies indicates that all three proteins, PMCA4, eNOS and CAV-1, are in a complex at high $[Ca^{2+}]_c$ in CAP sperm and more intensely with AR sperm. It should be noted that a CAV-1 band, the weakest in Fig. 1D, is seen in UNCAP proteins in the absence of an eNOS band. This could indicate that an undetectable small number of eNOS molecules are likely to be co-precipitated with the anti-PMCA4 antibodies in UNCAP proteins. The finding that anti-PMCA4 antibodies can Co-IP CAV-1 in the absence of appropriate binding motifs for PMCA4 and CAV1 indicates that the interaction is not direct.

To detect direct protein interactions between PMCA4 and the NOSs in the complex, FRET assays were performed. In Fig. 2A post-bleaching, compared to pre-bleaching, fluorescence intensities for the PMCA4-nNOS pair were shown to increase significantly ($P<0.05$) in CAP, but not UNCAP, sperm. This indicates an absence of donor (nNOS) de-quenching in the presence of the acceptor molecule (PMCA4) in UNCAP sperm. De-quenching of nNOS in CAP sperm is seen in Fig. 2B which reveals multiple regions where FRET had occurred with higher post-bleaching fluorescence intensity. These observations differ from the Co-IP data, where interaction was seen in CAP and UNCAP sperm. When FRET efficiencies were calculated, they were 24% and 6% for CAP and UNCAP sperm, respectively (Fig. 2C).

These values are significantly (P<0.01) different and indicate that PMCA4 and nNOS are within 10 nm apart only in CAP sperm where the 20% threshold was reached (Bragdon et al., 2009).

For the PMCA4-eNOS pair, post-bleaching fluorescence intensities were shown to increase for both CAP and UNCAP sperm. The difference between pre- and post-bleaching intensities were shown to be significant for UNCAP (P<0.01) and highly significant (P<0.0001) for CAP sperm, indicating the occurrence of FRET for both (Fig. 3A–C). In Fig. 3B there is de-quenching of eNOS in the presence of PMCA4 at multiple regions, most intensely at the neck in CAP sperm. It should be noted that in some sperm, de-quenching was seen in the proximal principal piece. A comparison of FRET efficiency values, 35% and 24% for CAP and UNCAP, in Fig. 3D shows both to be above the 20% threshold, indicating that PMCA4 and eNOS are within 10 nm apart in both CAP and UNCAP sperm. However, the FRET efficiency is significantly (P<0.01) higher in CAP sperm (Fig. 3D), indicating that significantly more molecules are exhibiting FRET at elevated $Ca^{2+}]_c$. This finding for PMCA4-eNOS is consistent with the Co-IP results.

When NOS activity was analyzed in *Pmca4* null sperm at both low and high $[Ca^{2+}]_c$ in the UNCAP and CAP states it was strikingly greater in CAP, compared to that in WT littermates, as seen by peak shifts to the right in the graphs (Fig. 4A). There was a greater that 2-fold increase in fluorescence units for the median of each null population studied (Fig, 4A). *Jam-A* null sperm were also studied for NOS activity since they have significantly reduced PMCA4 activity (Aravindan et al., 2012). In WT sperm, NOS activity was shown to be tightly regulated at high $[Ca^{2+}]_c$ in CAP sperm, with the mean fluorescence units being <5% greater than that in UNCAP sperm. However, for *Jam-A* nulls the difference between CAP and UNCAP was 8-fold higher (40%) than in nulls (Fig. 4B).

When sperm were studied for the levels of $OONO^-$, as expected they were higher in WT CAP versus UNCAP where the median fluorescence units were ~60 and ~80 (Fig. 5c), while for *Pmca4* nulls the medians were ~120 and ~160 (Fig. 5d). Thus when WT and nulls were compared, UNCAP and CAP, the median fluorescence units for each increased ~2-fold for nulls versus WT sperm (Fig. 5a, b).

To determine if the elevated levels of OONO- in *Pmca4* null males might lead to oxidative stress that could damage germ cells, the TUNEL assay was performed on testicular sections from nulls and WT littermates. Significantly (P<0.0001) increased numbers of TUNEL-positive cells were detected in null males (Fig. 6). While the numbers of apoptotic cells in the interstitial spaces did not differ significantly (P>0.05) in nulls and WT, they did in spermatogonia (P<0.0001), spermatocytes (P<0.05) and spermatids (P<0.0001) (Fig. 6).

Discussion

PMCA4 and the NOSs Co-localize and Intimately Interact in Murine Sperm in a Ca^{2+}-dependent manner

While PMCA4 (Wennemuth et al., 2003; Aravindan et al., 2012) and nNOS (Herrero et al., 1996) have been localized in murine sperm on the head, over the acrosome, and on the

proximal principal piece, to our knowledge there have been no reported localizations of eNOS in this species. When the NOSs were localized in Fig. 1A, we show that nNOS is more abundant and more widely distributed on the sperm, being found in the distal principal piece where eNOS and PMCA4 do not reside. In the present study the pre- and post-bleaching images for the FRET data revealed the close interaction of PMCA4 and the NOSs on the sperm head, neck (Fig. 2,3), and on the proximal principal piece of the flagellum, reflecting their co-localization. This is the first report of the localization for eNOS in murine sperm (Fig. 1A, 3) and our results provide confirmation of that reported for nNOS by Herrero et al. (1996).

These localizations in murine sperm are similar to what has been reported for nNOS and eNOS in human sperm (Herrero et al., 1996; O'Bryan et al., 1998; Andrews et al., 2015), where they were also shown to co-localize (Andrews et al., 2015). Interestingly in Fig. 3, for eNOS-PMCA4 in CAP sperm there is co-localization at the neck and intense interaction of the proteins, similar to the co-localization seen in humans (Andrews et al., 2015). At this location in human sperm there is a Ca^{2+} store (Costello et al., 2009) and recently, with the use of Super-resolution structured illumination microscopy (SR-SIM) it has been proposed that such a store may also exist in the mouse at the neck (Al-Dossary et al., 2015). These spatial relationships may be of functional significance.

In the present study we show, via reciprocal Co-IP, that PMCA4 binds to eNOS only when the $[Ca^{2+}]_c$ is elevated in CAP and AR sperm (Fig. 1C, D). The finding that the band seen in AR sperm [where there is a greater Ca^{2+} influx than in CAP sperm (Fraser, 1987; de Lamirande et al., 1997)] is more intense (Fig. 1C) is consistent with Ca^{2+}-dependency of the binding. Similar associations of PMCA4 and eNOS in Co-IP have recently been reported for human AR sperm, compared to UNCAP ones (Andrews et al., 2015), underscoring the interaction when $[Ca^{2+}]_c$ is elevated and the efflux pump is active. On the other hand nNOS-PMCA4 interaction in Co-IP occurred in CAP and AR as well as UNCAP sperm. The interaction in UNCAP proteins was not consistent: in the anti-nNOS IP binding occurred preferentially, compared to that in CAP and AR, while for the anti-PMCA4 IP it was marginal compared to CAP. The difference in the behavior of the NOSs, which was also noted for human sperm (Andrews et al., 2015), may reside in the fact that nNOS molecules are far more abundant and available for interaction and that they exist in both membrane-associated insoluble and soluble forms (Matsumoto et al., 1993). Together, these observations with Co-IP underscore the existence of molecular associations of PMCA4 and the NOSs.

In general, the Co-IP data were confirmed by FRET assays which are extremely efficient in detecting direct molecular interactions. FRET efficiencies revealed that for both PMCA4-nNOS and PMCA4-eNOS pairs, direct interactions preferentially occur in CAP sperm (Fig. 2,3), as seen in human sperm for the PMCA4-eNOS pair (Andrews et al., 2015). For UNCAP sperm, direct interaction occurred only for the PMCA4-eNOS pair. This is consistent with an earlier report that in UNCAP sperm PMCA4 binds preferentially to CASK via its PDZ ligand at the C-terminus (Aravindan et al., 2012). Thus PMCA4's PDZ ligand is unavailable to interact with the PDZ domain of nNOS in UNCAP sperm, and therefore binding to the PDZ domains on nNOS and CASK occurs sequentially (Aravindan

et al., 2012). However, it has been suggested that PMCA4 whose active form is a dimer (Di Leva et al., 2008) could interact simultaneously with the PDZ domains of nNOS and CASK via each monomer (Andrews et al., 2015). This would be consistent with the finding that in Co-IP strong PMCA4-nNOS interaction occurs in UNCAP sperm when $[Ca^{2+}]_c$ is basal as well as in elevated $[Ca^{2+}]_c$ in CAP and AR sperm.

Elevated NO levels Mediate Motility defects in Pmca4 Null Sperm

Based on the inhibitory effect of PMCA4-NOS interaction on NOS activity in somatic cells (Schuh et al., 2001; Holton et al., 2010), we proposed that a similar down-regulation of NOS activity would accompany the interaction of these proteins in CAP sperm in order to maintain optimal physiological levels of NO. This down-regulation is necessary since the NOSs are rapidly activated in the presence of elevated $[Ca^{2+}]_c$ (Knowles and Moncada, 1994). To assess the importance of the PMCA4-NOS interaction on NO regulation, NOS levels were determined in *Pmca4* null and *Jam-A* null sperm where PMCA4 activity is significantly decreased (Aravindan et al., 2012). The data in Fig. 4 show NOS activity levels that are elevated ~2-fold for both CAP and UNCAP *Pmca4* null sperm versus WT, while for *Jam-A* nulls the elevation was seen only in CAP sperm, indicating PMCA4's role in regulating NOS activity and NO levels in sperm. In human sperm, elevated levels of NO are well-known to play a major role in AS and male infertility (Nobunaga et al., 1996, Ramya et al., 2011; Salvolini et al., 2012) and are likely to be the cause of the *Pmca4* null phenotype.

Since a primary effector of NO is OONO, we assayed $OONO^-$ levels and showed that for *Pmca4* null sperm, CAP and UNCAP, there was an ~2-fold increase in $OONO^-$, compared to WT (Fig. 5). This is consistent with increased levels of NO in null sperm. Elevated levels of the highly reactive peroxynitrite are known to exert detrimental effects via cellular toxicity. In Fig. 6 we show that the testes of *Pmca4* nulls have elevated levels of apoptotic cells which resided mainly among the germ cells. This is consistent with the finding that *Pmca4* transcripts are expressed in spermatogonia, spermatocytes, and spermatids in the murine testes (Patel et al., 2013). Thus, although the sperm numbers in *Pmca4* null sperm are not decreased (Schuh et al., 2004; Okunade et al., 2004), due to the apoptotic activity, the elevated level of $OONO^-$ in these sperm could lead to increased DNA damage.

By reacting with both polyunsaturated fatty acids (PUFA) and amino acid residues in cell membranes, elevated levels of $OONO^-$ lead to lipid peroxidation and other pathological effects (Zylinksa and Soszynski, 2000); Zaidi and Michealis, 1999). As the mammalian sperm membrane is rich in PUFA, it is prone to lipid peroxidation which leads to a loss of sperm motility (Hellstrom et al., 1994). Thus our results support our hypothesis that oxidative stress underlies the mechanism involved in motility loss in PMCA4's absence in *Pmca4* nulls or its reduced activity in *Jam-A* nulls.

PMCA4 is involved in a Quaternary Signaling Complex that regulates Motility

Based on our results we propose a model for a novel quaternary complex (CAV1-eNOS-PMCA4b-nNOS; Fig. 7) in which PMCA4's inhibitory effect on NOS activity results from its Ca^{2+} extrusion role which creates a local environment with low $[Ca^{2+}]_c$ (Holton et al., 2007, 2010, Oceandy et al., 2007), when $[Ca^{2+}]_c$ is globally high. Of the two isoforms of

PMCA4, 4a and 4b, the latter is able to engage simultaneously in a PDZ domain-mediated interaction with nNOS and an interaction with eNOS at its larger cytoplasmic loop, the catalytic core (aa 428–651), while eNOS interacts with CAV-1 (Dhillion et al., 2003) (Fig. 7A). Importantly, PMCA4's activity must be inhibited when $[Ca^{2+}]_c$ is globally low to prevent suboptimal Ca^{2+} and NO levels which are detrimental to sperm (Ramya et al., 2011), as NO is involved in a variety of functional activities (Herrero et al., 2001).

Thus as $[Ca^{2+}]_c$ is reduced, conformational changes in nNOS and CASK appear to favor nNOS's release from PMCA4b which then binds to CASK (Fig. 7B). It should be noted that nNOS is known to exist in both an insoluble and a soluble form (Matsumoto et al., 1993), and the latter is able to enter other microdomains after release from PMCA4b. On the other hand, CASK is known to undergo a Ca^{2+}-dependent conformational change (Funke et al., 2005). Its type II PDZ domain which has a higher affinity for JAM-A's type II PDZ ligand when Ca^{2+} levels are elevated, releases JAM-A in low $[Ca^{2+}]_c$ and is available to bind to PMCA4 in UNCAP sperm. Since eNOS, unlike nNOS and CASK, appears to have no competitive binding for PMCA4 it retains its binding with PMCA4 at low $[Ca^{2+}]_c$ in UNCAP sperm (Fig. 3A, 7B) where its interaction with CAV-1 is also inhibitory (Ju et al., 1997).

Although PMCA pumps are known to be auto-inhibited (Di Leva et al., 2008), the interaction of PMCA4 with CASK in sperm at low $[Ca^{2+}]$c (Aravindan et al., 2012) may be required to maintain its inactivation. This PMCA4b-CASK complex which occurs promiscuously between the type I PDZ ligand of PMCA4b and CASK's type II PDZ domain (DeMarco and Strehler, 2001) maintains the inactivity of the pump and becomes easily dissociated when $[Ca^{2+}]_c$ rises. It should also be noted that CASK, which has a CaM kinase II domain (Funke et al., 2005), is known to phosphorylate recruited targets (Mukherjee et al., 2008), and phosphorylation inhibits activity of PMCA family members (Di Leva et al., 2008). Importantly, our model is consistent with the reported evidence for a Ca^{2+}/CaM/CaMKII signaling pathway that is involved in the regulation of sperm motility in the sperm principal piece (Schlingmann et al., 2007) where PMCA4 and CASK (Aravindan et al., 2012) and the NOSs have been localized. Further study is warranted to determine if PMCA4 is phosphorylated by CASK when the $[Ca^{2+}]$c is basal to maintain its inactivity.

In the absence of the pump in *Pmca4* null sperm (Fig. 7C), $[Ca^{2+}]_c$ is elevated beyond physiological levels, resulting in increased NOS activity, NO, and $OONO^-$ levels with adverse downstream effects of the latter. The highly reactive $OONO^-$ could induce oxidative stress, ultimately impacting the integrity of the sperm's genome (Aitken et al. (2014). This correlates with the significantly ($P<0.001$) increased levels of apoptotic germ cells detected in *Pmca4* null testes, and is consistent with that seen in smooth muscle cells from the portal vein of nulls (Okunade et al., 2004). It should be noted that in addition to elevated NO levels, elevated Ca^{2+} levels which result in sequestration of Ca^{2+} in the mitochondria of *Pmca4* null sperm (Okunade et al., 2004) could also impact motility of *Pmca4* null sperm by affecting mitochondrial membrane potential and ATP level, the latter via inhibition of dynein-ATPase (Peralta-Arias et al., 2015).

Conclusions

We conclude that in murine, as in human, sperm PMCA4 and the constitutive NOSs are interacting partners: eNOS binds preferentially when the $[Ca^{2+}]_c$ is elevated and the pump is active. While FRET data show nNOS also to bind preferentially at elevated $[Ca^{2+}]_c$, co-IP data show it to bind at both elevated and basal $[Ca^{2+}]_c$, possibly due to its greater abundance and its existence in both insoluble and soluble forms. PMCA4-NOS interaction down-regulates NOS activity and we have put forth a model of a quaternary signaling complex involving CAV-1 (CAV-1-eNOS-PMCA4-nNOS) that is responsible for the regulation of NO. Thus PMCA4 co-ordinates both Ca^{2+} and NO signaling in mammalian sperm. In the absence of PMCA4 in *Pmca4* null sperm, the loss of motility is likely to be mediated by elevated levels of NO and $OONO^-$ and the potential pathological effects which include apoptosis/DNA damage detected in germ cells. The cytotoxic effects of increased levels of $OONO^-$ include lipid peroxidation which may play a crucial role in the loss of motility in *Pmca4* null sperm.

Acknowledgments

We are grateful for Emily Jacobson and Pradeepthi Bathala for assisting with the co-immunoprecipitation assays. A part of the work was submitted by KEO, in partial fulfillment for the Master's degree.

Grant Sponsor NIH Grant Number -RO3HD073523

Grant sponsor NIH NCRR Grant Number 2P20 RR015588-09

Literature cited

Aitken RJ, Smith TB, Jobling MS, Baker MA, De Iuliis GN. Oxidative stress and male reproductive health. Asian J Androl. 2014; 16:31–38. [PubMed: 24369131]

AL-Dossary AA, Bathala P, Caplan JL, Martin-DeLeon PA. Oviductosome-Sperm Membrane Interaction in Cargo Delivery: Detection of fusion and underlying Molecular Players using 3D Super-Resolution Structured Illumination Microscopy (SR-SIM). J Biol Chem. 2015; 290:17710–17723. [PubMed: 26023236]

Andrews RE, Galileo DS, Martin-DeLeon PA. Plasma Membrane Ca^{2+}-ATPase 4 (MCA4): Interaction with constitutive nitric oxide synthases in Human Sperm and Prostasomes which carry Ca^{2+}/CaM-dependent serine kinase (CASK). Mol Hum Reprod. 2015; 21:832–843. [PubMed: 26345709]

Aravindan GR, Fomin VP, Naik UP, Modelski MJ, Naik MU, Galileo DS, Duncan RL, Martin-DeLeon PA. CASK interacts with MCA4b and JAM-A on the mouse sperm flagellum to regulate Ca2+ homeostasis and motility. J Cell Physiol. 2012; 227:3180–3150.

Bragdon B, Thinakaran S, Bonor J, Underhill TM, Petersen NO, Nohe A. FRET reveals novel protein-receptor interaction of bone morphogenetic proteins receptors and adaptor protein 2 at the cell surface. Biophys J. 2009; 97:1428–1435. [PubMed: 19720031]

Bragdon B, Thinakaran S, Moseychuk O, King D, Young K, Litchfield DW, Petersen NO, Nohe A. Casein kinase 2 beta-subunit is a regulator of bone morphogenetic protein 2 signaling. Biophys J. 2010; 99:897–904. [PubMed: 20682268]

Costello S, Michelangeli F, Nash K, Lefievre L, Morris J, Machado-Oliveira G, Barratt C, Kirkman-Brown J, Publicover S. Ca2+-stores in sperm: their identities and functions. Reroduction. 2009; 138:425–437.

de Lamirande E, Leclerc P, Gagnon C. Capacitation as a regulatory event that primes spermatozoa for the acrosome reaction and fertilization. Mol Hum Reprod. 1997; 3:175–194. [PubMed: 9237244]

DeMarco SJ, Strehler EE. Plasma membrane Ca2+-ATPase isoforms 2b and 4b interact promiscuously and selectively with members of the membrane-associated guanylate kinase family of PDZ

(SD95/Dlg/ZO-1) domain-containing proteins. J Biol Chem. 2001; 276:21594–21600. [PubMed: 11274188]

Deng X, Czymmek K, Martin-DeLeon PA. Biochemical Maturation of Spam1 (PH-20) during Epididymal transit of the Mouse Sperm involves Modifications of N-linked oligosaccharides. Mol Reprod Dev. 1999; 55:196–206.

Dhillon B, Badiwala MV, Li S-H, Li R-K, Weisel RD, Mickle DAG, Fedak Paul WM, Rao V, Verma S. Caveolin: A key target for modulating nitric oxide availability in health and disease. Mol Cell Biochem. 2003; 247:101–109. [PubMed: 12841637]

Di Leva F, Domi T, Fedrizzi L, Lim D, Carafoli E. The plasma membrane Ca2+ ATPase of animal cells: structure, function and regulation. Arch Biochem Biophys. 2008; 476:65–74. [PubMed: 18328800]

Fraser LR. Minimum and maximum extracellular Ca^{2+} requirements during mouse sperm capacitation and fertilization. J Reprod Fertil. 1987; 81:77–89. [PubMed: 3668962]

Funke L, Dakoji S, Bredt DS. Membrane-associated guanylate kinases regulate adhesion and plasticity at cell junctions. Ann Rev Biochem. 2005; 74:219–245. [PubMed: 15952887]

Hellstrom WJG, Bell M, Wang R, Sikka SC. Effect of sodium nitroprusside on sperm motility, viability, and lipid peroxidation. Fertil Steril. 1994; 61:1117–1122. [PubMed: 8194627]

Herrero MB, Gagnon C. Nitric oxide. A Novel Mediator of Sperm Function: J Androl. 2001; 22:349–356. [PubMed: 11330633]

Herrero MB, Perez Martinez S, Viggiano JM, Polak JM, Gimeno MF. Localization by indirect immunofluorescence of nitric oxide synthase in mouse and human spermatozoa. Reprod Fertil Dev. 1996; 8:931–934. [PubMed: 8876053]

Herrero MB, de Lamirade E, Gagnon C. Tyrosine nitration in human spermatozoa: a physiological function of peroxynitrite, the reaction product of nitric oxide and superoxide. Mol Hum Reprod. 2001; 7:913–919. [PubMed: 11574660]

Herrick SB, Schweissinger DL, Kim SW, Bayan KR, Mann S, Cardullo RA. The acrosomal vesicle of mouse sperm is a calcium store. J Cellular Physiol. 2005; 202:663–671. [PubMed: 15389568]

Holton M, Yang D, Wang W, Mohamed TM, Neyses L, Armesilla AL. The interaction betweenendogenous calcineurin and the plasma membrane calcium-dependent ATPase is isoform specific in breast cancer cells. FEBS Lett. 2007; 581:4115–4119. [PubMed: 17689535]

Holton M, Mohamed TM, Oceandy D, Wang W, Lamas S, Emerson M, Neyses L, Armesilla AL. Endothelial nitric oxide synthase activity is inhibited by the plasma membrane calcium ATPase in human endothelial cells. Cardiovasc Res. 2010; 87:440–448. [PubMed: 20211863]

Ju H, Zou R, Venema VJ, Venema RC. Direct interaction of endothelial nitric-oxide synthase and caveolin-1 inhibits synthase activity. J Biol Chem. 1997; 272:18522–18525. [PubMed: 9228013]

Knowles RG, Moncada S. Nitric oxide synthases in mammals. Biochem J. 1994; 298:249–258. [PubMed: 7510950]

Matsumoto T, Nakane M, Pollock JS, Kuk JE, Förstermann U. A correlation between soluble brain nitric oxide synthase and NADPH-diaphorase activity is only seen after exposure of the tissue to fixative. Neuroscience Lett. 1993; 155:61–64.

Modelski MJ, Menlah G, Wang Y, Dash S, Wu K, Galileo DS, Martin-DeLeon PA. Hyaluronidase 2: A Novel Germ Cell Hyaluronidase with Epididymal Expression and Functional Roles in Mammalian Sperm. Biol Reprod. 2014; 91:1–11.

Mukherjee K, Sharma M, Urlaub H, Bourenkov GP, John R, Sudhof TC, Wahl MC. CASK functions as a Mg^{2+}-dependent neurexin kinase. Cell. 2008; 133:328–339. [PubMed: 18423203]

Nobunaga T, Tokugawa Y, Hashimoto K, Kubota Y, Sawai K, Kimura T, Shimoya K, Takemura M, Matsuzaki N, Azma C, et al. Elevated nitric oxide concentration in the seminal plasma of infertile males: nitric oxide inhibits motility. Am J Reprod Immunol. 1996; 36:193–197. [PubMed: 8911625]

Oceandy D, Stanley PJ, Cartwright EJ, Neyses L. The regulatory function of plasma membrane Ca2+-ATPase (PMCA) in the heart. Biochem Soc Trans. 2007; 35:927–930. [PubMed: 17956248]

Okunade GW, Miller ML, Pyne GJ, Sutliff RL, O'Connor KT, Neumann JC, Andringa A, Miller DA, Prasad V, Doetschman T, et al. Targeted ablation of plasma membrane Ca2+ -ATPase (PMCA) 1 and 4 indicates a major housekeeping function for PMCA1 and a critical role in hyperactivated

sperm motility and male fertility for PMCA4. J Biol Chem. 2004; 279:33742–33750. [PubMed: 15178683]

O'Bryan MK, Zini A, Cheng CY, Schlegel PN. Human sperm endothelial nitric oxide synthase expression: correlation with sperm motility. Fertil Steril. 1998; 70:1143–1147. [PubMed: 9848308]

Patel R, Al-Dossary AA, Stabley DL, Barone C, Galileo DS, Strehler EE, Martin-DeLeon PA. Plasma membrane Ca2+-ATPase 4 in murine epididymis: secretion of splice variants in the luminal fluid and a role in sperm maturation. Biol Reprod. 2013; 89:1–11.

Peralta-Arias RD, Vivenes CY, Camejo MI, Pinero S, Proverbio T, Martinez E, Marin R, Proverbio F. ATPases, ion exchangers and human sperm motility. Reproduction. 2015; 149:475–484. [PubMed: 25820902]

Ramya T, Man Mohan M, Devabrata S, Nandan D, Sandeep M. Altered levels of seminal nitric oxide, nitric oxide synthase, and enzymatic antioxidants and their association with sperm function in infertile subjects. Fertil Steril. 2011; 95:135–140. [PubMed: 20684956]

Salvolini E, Buldreghini E, Lucarini G, Vignini A, Di Primio R, Balercia G. Nitric oxide synthase and tyrosine nitration in idiopathic asthenozoospermia: an immunohistochemical study. Fertil Steril. 2012; 97:554–550. [PubMed: 22244784]

Schlingmann K, Michaut MA, McElwee JL, Wolff CA, Travis AJ, Turner RM. Calmodulin and CaM KII in the sperm principal piece: evidence for a motility-related calcium/calmodulin pathway. J Androl. 2007; 28:706–716. 2007. [PubMed: 17460096]

Schuh K, Cartwright EJ, Jankevics E, Bundschu K, Liebermann J, Williams JC, Armesilla AL, Emerson M, Oceandy D, Knobeloch KP, et al. Plasma membrane Ca2+ ATPase 4 is required for sperm motility and male fertility. J Biol Chem. 2004; 279:28220–28226. [PubMed: 15078889]

Schuh K, Uldrijan S, Gambaryan S, Roethlein N, Neyses L. Interaction of the plasma membrane Ca^{2+} pump 4b/CI with the Ca^{2+}/calmodulin-dependent membrane-associated kinase CASK. J Biol Chem. 2003; 278:9778–9783. [PubMed: 12511555]

Schuh K, Uldrijan A, Telkamp M, Rothlein N, Neyses L. The plasma membrane calmodulin-dependent calcium pump: a major regulator of nitric oxide synthase 1. J Cell Biol. 2001; 273:18693–18696.

Setsukinai K-I, Urano Y, Kakinuma K, Majima HJ, Nagano T. Development of novel fluorescence probes that can reliably detect reactive oxygen species and distinguish specific species. J Biol Chem. 2003; 278:3170–3175. [PubMed: 12419811]

Shao M, Ghosh A, Cooke VG, Naik UP, Martin-DeLeon PA. JAM-A is present in mammalian spermatozoa where it is essential for normal motility. Dev Biol. 2008; 313:246–255. [PubMed: 18022613]

Travis AJ, Merdiushev T, Vargas LA, Jones BH, Purdon MA, Nipper RW, Galatioto J, Moss SB, Hunnicutt GR, Kopf GS. Expression and localization of Caveolin-1 and the presence of membrane raftsin mouse and guinea pig sperm. Dev Biol. 2001; 240:599–610. [PubMed: 11784086]

Wennemuth G, Babcock DF, Hille B. Calcium clearance mechanisms of mouse sperm. J Gen Physiol. 2003; 122:115–128. [PubMed: 12835474]

Zaidi A, Michealis ML. Effects of reactive oxygen species on brain synaptic plasma membrane Ca^{2+}-ATPase. Free Radical Biol Med. 1999; 27:810–821. [PubMed: 10515585]

Zhang H, Martin-DeLeon PA. Mouse Epididymal Spam1 (PH-20) Is Released in the Luminal Fluid with its Lipid Anchor. J Androl. 2003; 24:51–58. [PubMed: 12514083]

Zini A, O'Bryan MK, Magid MS, Schlegel PN. Immunohistochemical localization of endothelial nitric oxide synthase in human testis, epididymis, and vas deferens suggests a possible role for nitric oxide in spermatogenesis, sperm maturation, and programmed cell death. Biol Reprod. 1996; 55:935–939. [PubMed: 8902202]

Zylinska L, Soszynski M. Plasma membrane Ca^{2+} -ATPase in excitable and non-excitable cells. Acta Biochimica Polonica. 2000; 47:529–539. [PubMed: 11310957]

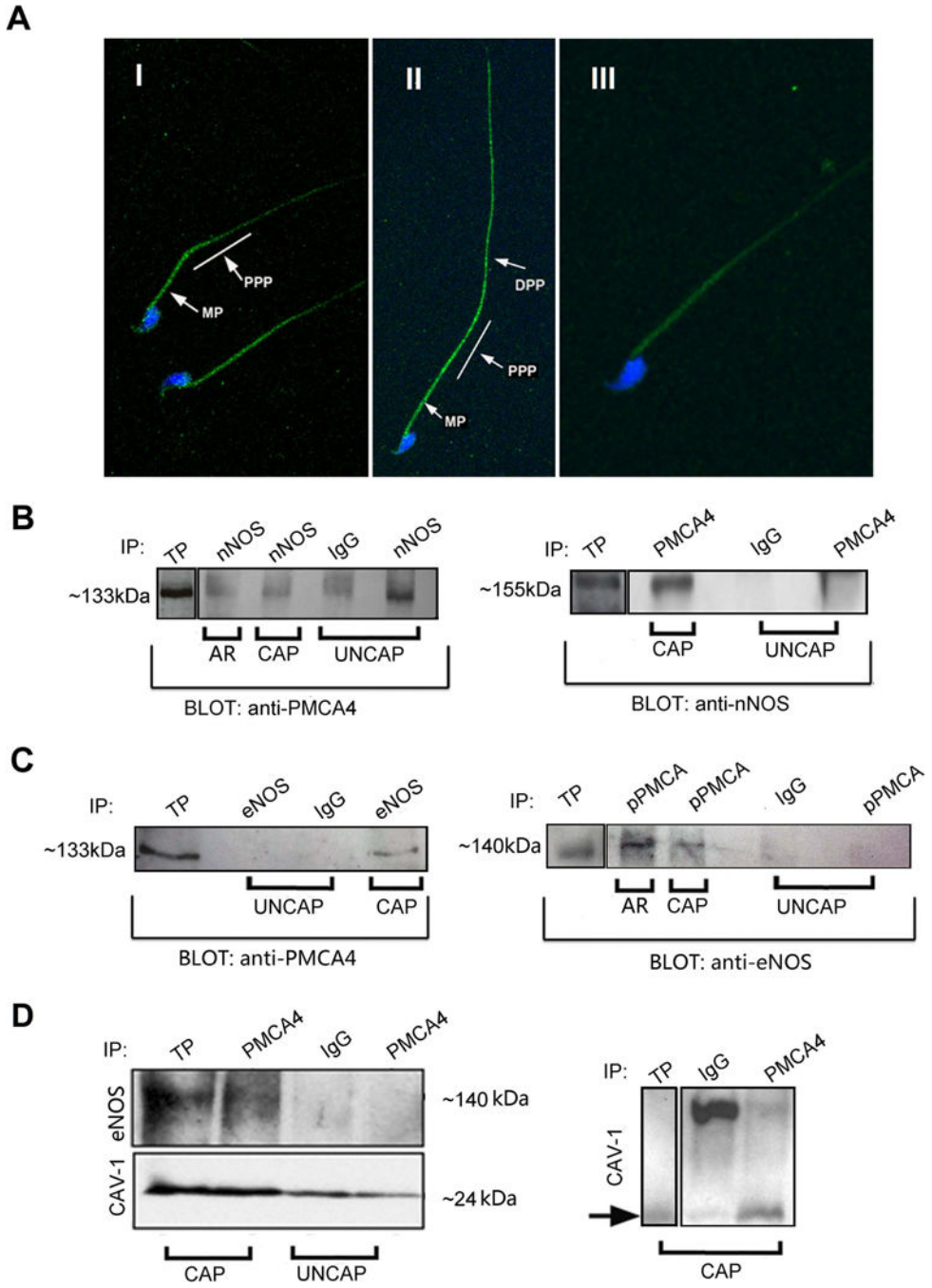

Fig. 1. nNOS is more abundant and more widely distributed than eNOS in murine sperm where reciprocal co-immunoprecipitation (Co-IP) reveals that the NOSs and PMCA4 interact

A) I) Indirect immunofluorescence using anti-eNOS antibodies show eNOS (green signal) on the head, the midpiece (MP), and the proximal principal piece (PPP). II) Anti-nNOS antibodies show nNOS in the distal principal piece (DPP) as well as the MP and PPP. III) The IgG control is seen with the blue DAPI staining in the head and only background fluorescence on part of the flagellum. **B)** Anti-nNOS antibodies co-precipitate a 133 kDa PMCA4 band in AR, CAP and UNCAP sperm, with the latter being most intense. The

positive control, total protein (TP), and the rabbit IgG negative control are shown. In the reciprocal Co-IP (right), anti-PMCA4 antibodies showed a stronger interaction of the 155 kDa nNOS band and PMCA4 in CAP versus UNCAP sperm, with the goat IgG negative control showing the specificity of the interaction. **C)** The 133 kDa PMCA4 band was seen in CAP sperm, but absent in UNCAP when anti-eNOS antibodies were used for the IP. In the reciprocal Co-IP (right) the 140 kDa eNOS band was detected in CAP, but not the UNCAP, samples. It was also detected in AR sperm where it is stronger than that in the CAP. **D)** Co-IP of eNOS and CAV1 with pan-PMCA4 antibodies in proteins extracted from sperm with high, but not low, $[Ca^{2+}]_{c.}$ After Co-IP of eNOS, the membrane was stripped and re-probed with anti-CAV-1 antibodies (lower panel). The ~24 kDa CAV-1 band was detected in TP and above control (IgG) level only at high $[Ca^{2+}]_c$ in CAP samples. At right, only CAP proteins were assayed and the blot for CAV-1 shows a strong band for anti-PMCA4 antibodies IP, but none for the IgG control. These images are representative of results from > 9 experiments and uncropped gels are shown as Supplementary Figures. In the Supplementary gel for 1B, there is a non-specific band above the target band.

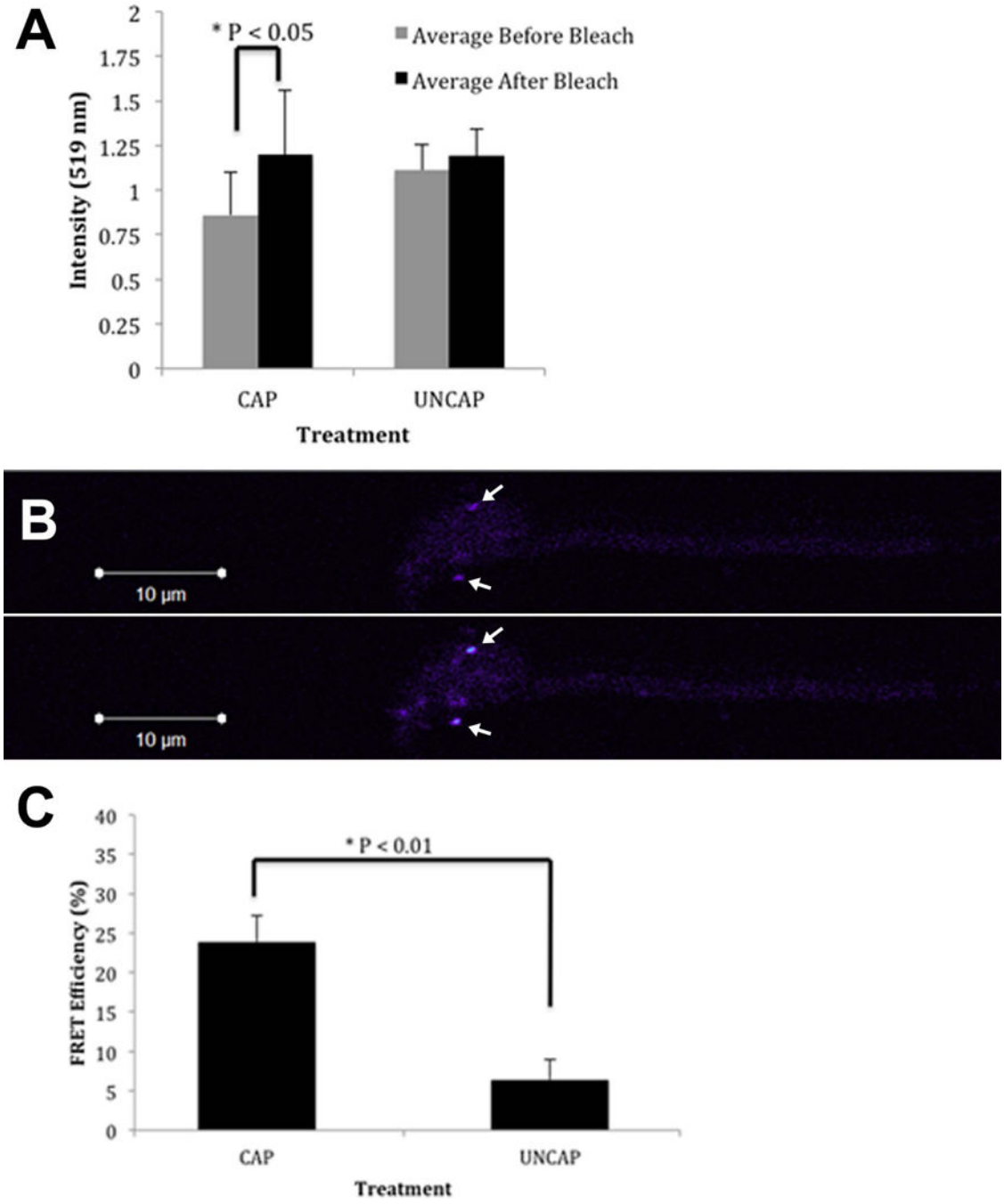

Fig. 2. Direct interaction of PMCA4 and nNOS in murine sperm was detected by FRET

A) Comparison of the fluorescence intensities in CAP and UNCAP sperm, immunostained for PMCA4 and nNOS, before and after bleaching. A significant ($P<0.05$) difference is seen only for CAP sperm, indicating that FRET had occurred only in CAP samples. **B)** Images of a CAP sperm immunostained for PMCA4 and nNOS, taken before (upper panel) and after (lower panel) bleaching, indicate that there are two regions on the head (white arrows) in the lower panel with increased fluorescence intensity where de-quenching of nNOS occurs in the presence of PMCA4. These indicate areas where the molecules are within 10 nm apart

and are exhibiting FRET. **C)** FRET efficiencies for the PMCA4-nNOS pair were 24% and 6% for CAP and UNCAP sperm, indicating a significant ($P<0.01$) difference in the fraction of donor molecules (nNOS) exhibiting FRET (with UNCAP sperm falling below the 20% threshold). A total of 10 cells and 20 images/cell were analyzed for each group. Error bars represent standard errors (±SEM).

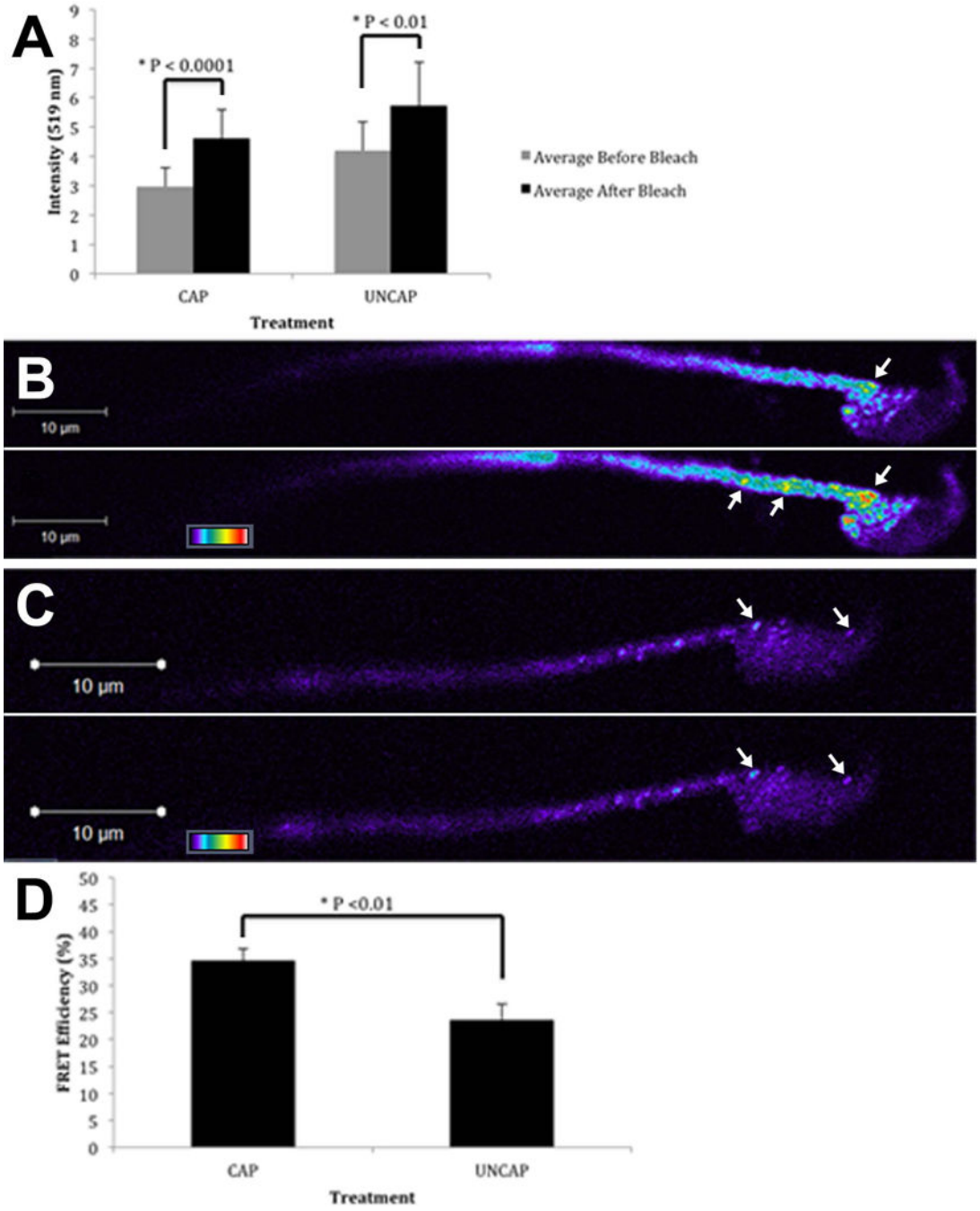

Fig. 3. Direct interaction of PMCA4 and eNOS in murine sperm was detected by FRET

A) Post-bleaching fluorescence intensities were significantly higher than pre-bleaching intensities after complete acceptor bleaching for both CAP ($P<0.0001$) and UNCAP ($P<0.01$) sperm, indicating the molecules are within 10 nm apart and therefore are exhibiting FRET. **B)** CAP sperm showing increase in donor fluorescence (white arrows) on the head and midpiece after complete acceptor bleaching (lower panel), compared to that in the pre-bleaching event (upper panel). The color spectrum shows warmer colors from left to right. In the lower panel increased fluorescence intensity is seen at the neck, as indicated by the

warmer colors. **C)** UNCAP sperm showing two areas with increase in donor fluorescence (white arrows), or de-quenching, after complete acceptor bleaching (lower panel), compared to that in the pre-bleaching event (upper panel). **D)** The average FRET efficiency for CAP (35%) was significantly ($P<0.01$) higher than that for UNCAP (24%), indicating that significantly more molecules in CAP versus UNCAP sperm exhibited FRET. A total of 10 cells and 20 images/cell were analyzed for each group. Error bars represent standard errors (±SEM).

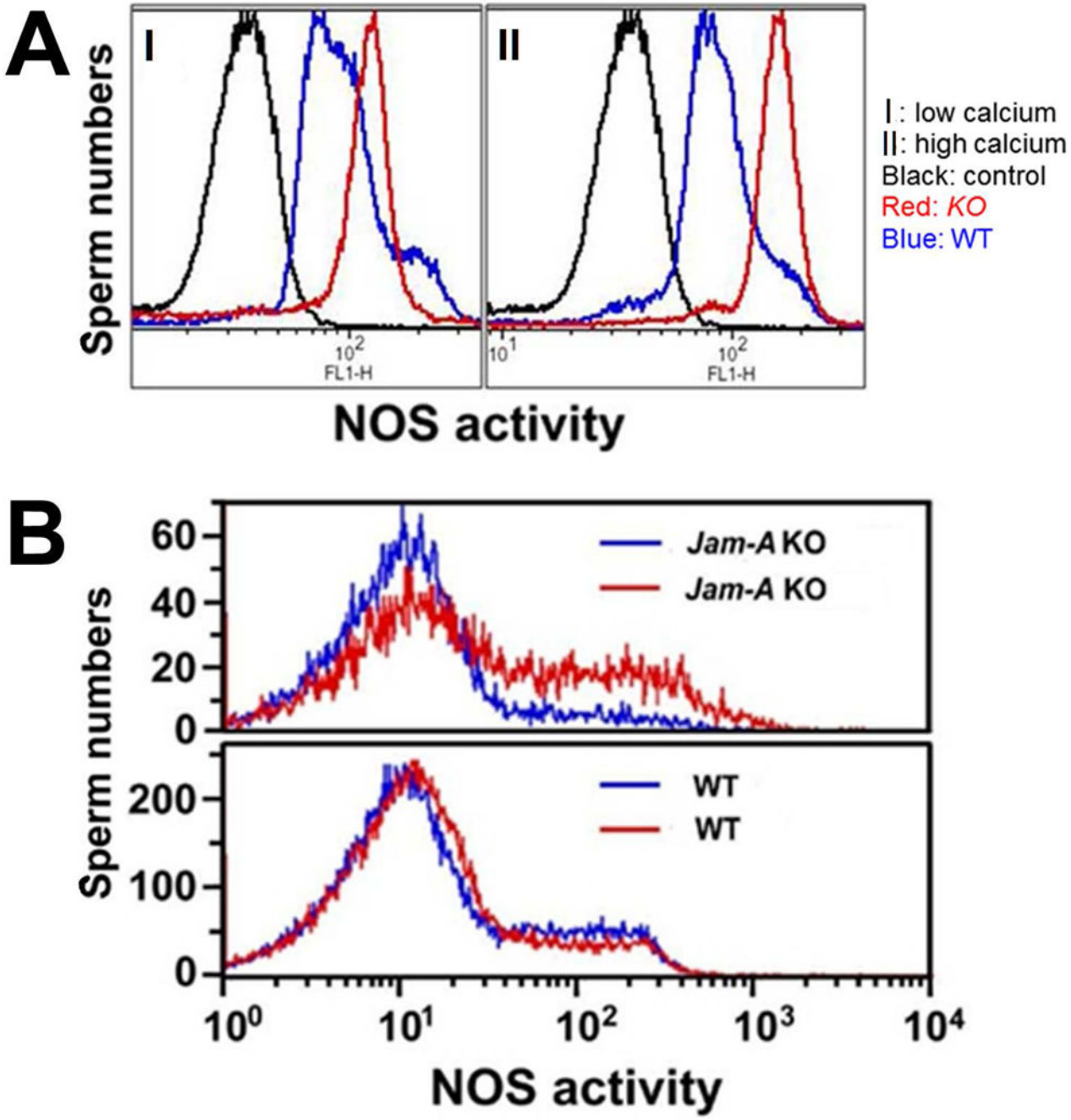

Fig. 4. Quantitative fluorescence, detected by flow cytometry, shows increased levels of NOS activity (NO bioavailability) in *Pmca4* and *Jam-A* null sperm

A) In UNCAP (I) and CAP (II) *Pmca4* null sperm (red) NOS activity is elevated, as seen by peak shifts in fluorescence intensities to the right and a >2-fold increase in the median intensity compared to WT (blue). Note that the shift is greater in CAP than UNCAP samples. The no-dye control is seen in black. ~50,000 cells were analyzed per sample. **B)** NOS activity is markedly (40%) higher in *Jam-A* null CAP (red) sperm compared to

UNCAP (blue) (upper panel). For WT (lower panel) the difference between CAP and UNCAP is <5%, indicating a tighter control in NOS activity.

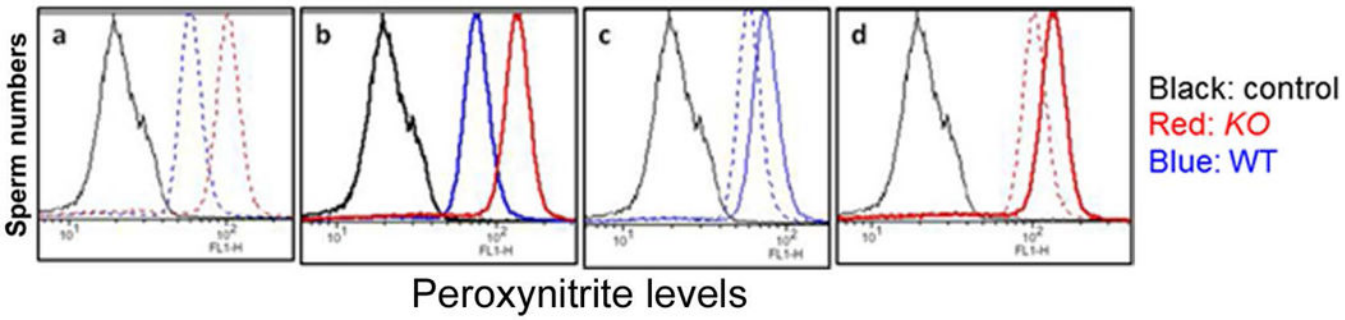

Fig. 5. Peroxynitrite ($OONO^-$) levels are increased in *Pmca4* null sperm

a) Quantitative fluorescence, reflecting $OONO^-$ levels, shows an ~2-fold increase in the median fluorescence intensity in UNCAP (broken lines) *Pmca4* sperm (red) over WT (blue). b) There is ~2-fold increase in the median fluorescence intensity in CAP (solid lines) *Pmca4* null sperm over WT. c) Fluorescence intensity units in CAP and UNCAP WT sperm are compared with d) *Pmca4* null sperm, showing a physiological role for its presence in capacitation. For each graph, the no-dye control is seen in black and for each sample 50,000 cells were analyzed.

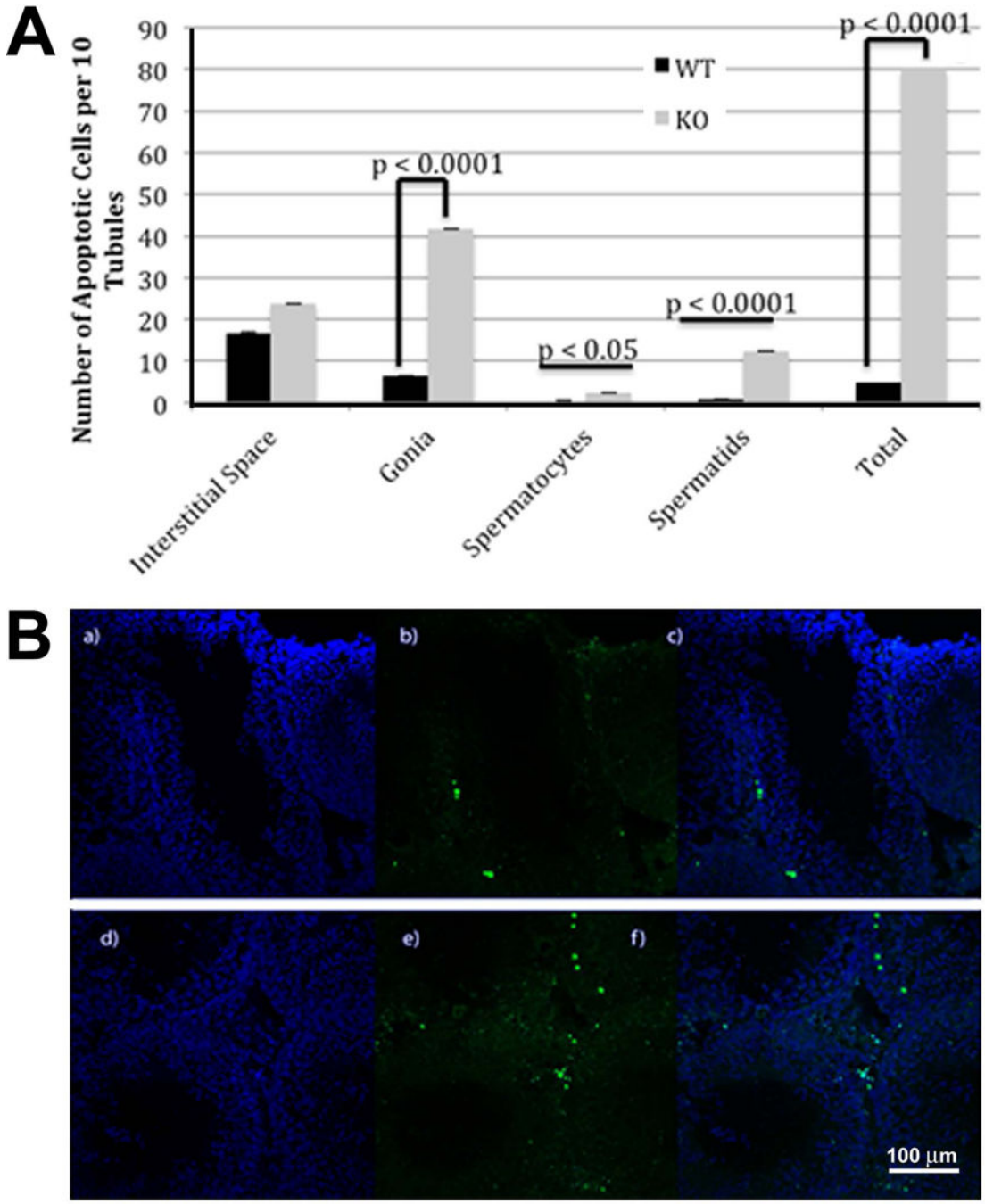

Fig. 6. *Pmca4* null males have increased numbers of apoptotic cells in the testis

A) TUNEL-positive cells in the testis are significantly (P<0.0001) increased compared to age-matched littermates. Apoptotic cells varied in different cell types: there was no significant (P>0.05) difference between cells in the interstitial space in nulls versus WT, while the difference was significant for spermatogonia (P<0.0001), spermatocytes (P<0.05), and spermatids (P<0.0001). **B)** Representative confocal images of testis sections showing TUNEL-positive cells. DAPI stained nuclei (a), fluorescein stained apoptotic cells (b), and a composite (c) in testes sections of wild-type mice where the majority of apoptotic cells are

in the interstitial space. The nuclei (d), apoptotic cells (e), and a composite (f) of the sections of *Pmca4* null mice show the majority of apoptotic cells in the spermatogonia.

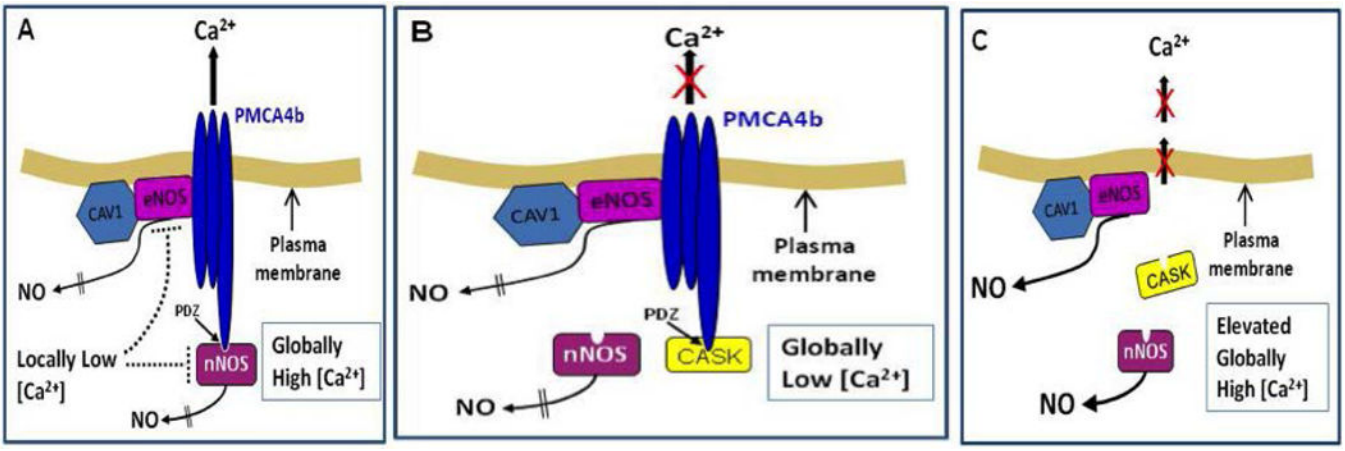

Fig. 7. Based primarily on direct interactions from the FRET data, a model of NO regulation in sperm is proposed: A quaternary signaling complex controls normal sperm motility and in the absence of PMCA4, motility is lost

In CAP sperm at high $[Ca^{2+}]_c$ **(A)**, PMCA4b's efflux role inhibits the NOSs, by creating microdomains of locally low $[Ca^{2+}]_c$. At low $[Ca^{2+}]_c$ in UNCAP sperm **(B)**, PMCA4b releases nNOS and binds CASK and its inactivation is maintained. Soluble nNOS is able to leave the PMCA4 microdomain and enter other microdomains. In PMCA4b's absence, $[Ca^{2+}]_c$ is elevated non-physiologically (**C**), NOSs are over-activated, resulting in increased NO levels followed by increased $OONO^-$ levels and detrimental downstream effects, with loss of sperm motility.